

# Quantum chemical and molecular docking studies of boron-doped and reduced graphene oxide supported nanocomposite

Sabeeha Jabeen<sup>1,2</sup>, Shristi Modanwal<sup>3</sup>, Nidhi Mishra<sup>3</sup>, Vasi Uddin Siddiqui<sup>4</sup>,  
Shashi Bala<sup>2</sup>, Tahmeena Khan<sup>1\*</sup>

<sup>1</sup>Department of Chemistry, Integral University, Uttar Pradesh, India.

<sup>2</sup>Department of Chemistry, University of Lucknow, Uttar Pradesh, India.

<sup>3</sup>Department of Applied Sciences, Indian Institute of Information Technology, Uttar Pradesh, India.

<sup>4</sup>Department of Mechanical and Manufacturing Engineering, Universiti Putra Malaysia, UPM Serdang, Darul Ehsan, Malaysia.

\*Corresponding author: [tahminakhan30@yahoo.com](mailto:tahminakhan30@yahoo.com)

## SHORT COMMUNICATION

Received:  
30 November 2023  
Revised:  
24 January 2024  
Accepted:  
03 February 2024  
Published online:  
30 March 2024

© The Author(s) 2024

## Abstract:

Nanocomposites have attracted great attention due to their outstanding properties compared to bulk materials for many applications in various fields. However, their computational studies for property exploration are still at a stage of infancy. So far very few studies have been attempted to study the quantum chemical parameters of nanocomposites. This article, reports the density functional theory (DFT) calculations and molecular docking studies to explain important properties of boron-doped and reduced graphene oxide (rGO) supported nanocomposite (B-CuO/rGO). Parameters including highest occupied molecular orbital (HOMO) and lowest occupied molecular orbital (LUMO), energy gap ( $\Delta E$ ), absolute hardness ( $\eta$ ), absolute softness ( $\sigma$ ), absolute electronegativity ( $\chi$ ), chemical potential ( $\mu$ ), global electrophilicity ( $\omega$ ), and additional electronic charge ( $\Delta N_{max}$ ) were predicted. Molecular docking was performed against antimicrobial protein target localization of lipoproteins (LolA) (PDB i.d. 2W7Q) from *Pseudomonas aeruginosa* and a binding energy of -11.7 kcal/mol was obtained showing appreciable binding of the nanocomposite with the active site of the protein.

**Keywords:** B-CuO/rGO; DFT; HOMO/LUMO bandgap; Molecular docking; Nanocomposite

## 1. Introduction

Nanocomposites have received more attention due to their wide applications in different fields [1–3]. Perhaps the most widely used matrix for nanocomposite formulation doping and forming a composite with rGO, which has effective therapeutic and environmental applications [4]. The structural stability of rGO is attributed to its mechanical and optical properties [5]. The incorporation of metallic and non-metallic oxide-based nanoparticles (NPs) in the rGO matrix has gained attention due to their innumerable applications [6]. The antibacterial potential of graphene oxide (GO) and rGO has also been studied earlier. A previous study reported that rGO was found to be more toxic than

the GO against Gram-positive *Staphylococcus aureus* and Gram-negative *Escherichia coli*. Furthermore, the better antibacterial activity of the rGO was attributed to improved charge transfer between the bacteria and more sharpened edges of the rGO, during interaction. It was found that the cell membrane damage was caused by the direct contact of the bacteria with the extremely sharp edges of nanowalls [7]. Studies have also established that GO can have toxic effects on cells and organisms, particularly when it is present in high concentrations. However, the toxicity can vary depending on factors such as the size, shape, and surface chemistry, as well as the route of exposure. GO and rGO have been reported to enhance bacterial toxicity through enhanced

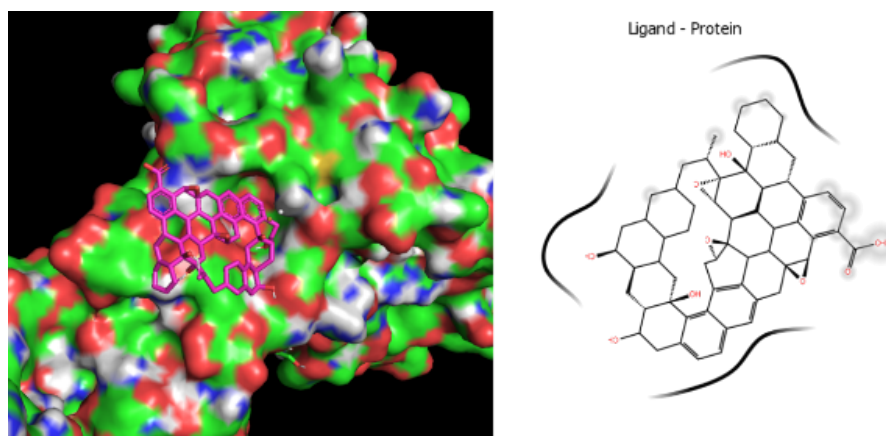


**Figure 1.** Interaction diagram of the docked complex.

production of ROS and cause loss of membrane integrity, and DNA damage in bacterial pathogens [8]. Quantum mechanical simulations can be used to assess the structural characteristics of new materials and also validate the experimental findings. As they are time-effective and accurate, they have received significant attention [9]. Density functional theory (DFT) based calculations have been used to explore important properties of nanocomposites. A relatively recent study reported a computational model for TiO<sub>2</sub> NPs using the DFT theory [10]. Computational resources use different theoretical algorithms for the calculation of various properties using semi-empirical DFT methods which have emerged as a prominent methodology for structure prediction and to understand mechanistic approaches [11, 12]. The DFT calculations may predict useful properties of nanomaterials, particularly their optical, catalytic, and magnetic properties. However, they are yet to be explored to be associated with their medicinal properties. Molecular docking is also a versatile method to study the interactions of the proposed compound against different targets. The interactions of nanostructures with macromolecular target proteins lead to physiological changes that cause different pathological phenotypes that need more exploration [13]. It is

pertinent to understand the protein-metal binding and the complex formed during the interaction between nanomaterials and the biomolecules and that has led to the utility of molecular docking which predicts the cooperation affinity of the protein-metal complex and also the hindrances and limitations where the binding is not feasible [14]. A recent study reported molecular docking studies of graphene-based nanocomposite against COVID-19 target proteins [15]. In this article, DFT and molecular docking studies of B-CuO/rGO nanocomposite are reported, which have not been explored previously. The authors have already reported the synthesis and characterization of the nanocomposite previously [6].

## 2. Material and methods

The DFT calculations were made using the MOPAC software. The interaction diagram was generated by Maestro. The compound was energetically minimized using Avogadro and the trajectory was generated by the MOPAC module. The results were analyzed using JMOL software. For molecular docking studies the 3D structure of *Pseudomonas aeruginosa* LolA (PDB ID: 2W7Q) was downloaded from the Protein Data Bank (PDB), and the 3D

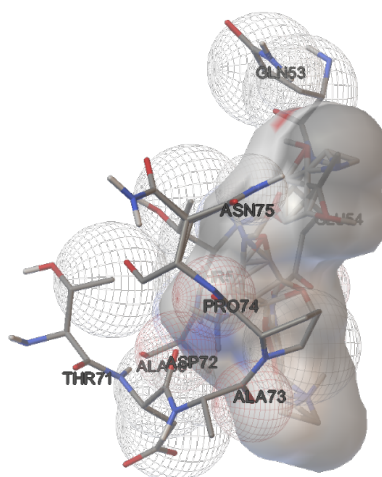


**Figure 2.** Interactions between LolA and gentamicin.

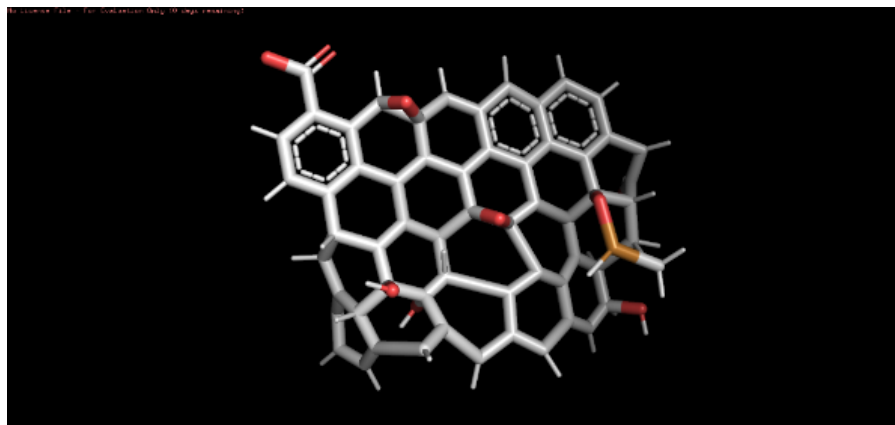


**Figure 3.** 3D structure of Boron doped CuO/rGO nanocomposite.

structure of the proposed B-CuO/rGO nanocomposite was drawn on ChemSketch. Molecular docking was done using Autodock 4.2, a freely available tool for docking analysis, on an Acer desktop with 8 GB of RAM and an Intel Core i5-4590 processor running at 3.30 GHz. PyMOL was used to visualize the docked structure.

### 3. Results and discussions

#### 3.1 Molecular docking

Molecular docking has emerged as an efficient tool to explore interesting drug candidates. The tool can also be used to predict the potential side effects or toxicities [16].

##### 3.1.1 Ligand and protein preparation

In molecular docking, the 3D structure of the ligand and target molecules are visualized first in their most preferred binding orientations and then the binding energy released upon formation of a stable complex is assessed [17]. The structure of the nanocomposite was drawn on Avogadro saved in .pdb format and utilized for docking analysis. The .pdb file of the nanocomposite was converted to .pdbqt format by the online conversion tool Open Babel [18]. The 3D structure of the target protein was downloaded from [www.rcsb.org](http://www.rcsb.org). The protein was prepared before docking and the hetero atoms were removed from the protein structure, also the proteins were checked for the missing atoms

and repaired. The protein was further prepared by adding hydrogen and charges, and the prepared protein was then saved in the .pdbqt format to be used for the docking. Lamarckian genetic algorithms (LGA) were used for docking calculations.

##### 3.1.2 Evaluation of the molecular docking results

The B-CuO/rGO nanocomposite exhibited a binding affinity of -11.7 kcal/mol against the selected protein. The binding energies of best-docked compounds usually range between -8.0 kcal/mol and -11.71 kcal/mol [19]. The interaction analysis of B-CuO/rGO docked conformers was done to know the binding pattern and probable interactions with LolA which is a periplasmic chaperon protein that can accept lipoproteins released from the inner membrane of a cell intended for the outer membrane [20]. LolA comprises of five different proteins viz. olA- LolE (1) LolCDE, an ATP-binding cassette transporter which newly synthesized lipoproteins that are destined for the outer membrane. LolCDE enhances the detachment of these lipoproteins from the inner membrane in the presence of LolA which forms a soluble complex with a lipoprotein to move it through the periplasmic space to reach LolB, a lipoprotein receptor [21]. The potential B- CuO/rGO nanocomposite binding sites in the protein pocket are shown in Figure 1. Molecular docking results showed that the nanocomposite can act as

**Table 1.** Parameters reflecting the reactivity and the stability of nanocomposite.

Parameters	DFT B-CuO/rGO
Ionization potential (eV)	7.246138
HOMO energy (eV)	-7.246
LUMO energy (eV)	-4.038
$\Delta E$ (ev)	3.208
$\chi$ (eV)	5.642
$\eta$ (eV)	1.604
$\sigma$ (eV)	0.62344
Pi (eV)	-5.642
$\omega$ (eV)	15.916082
$\Delta N_{max}$	3.5174

a ligand with the chosen microbial protein that acts as a receptor [15, 22].

The docking results of rGO were also compared with gentamicin (standard antibacterial drug). The docking score of gentamicin was found to be -9.67 kcal/mol, which was lower than the nanocomposite. Figure 2 shows the interactions between the selected protein and gentamicin.

### 3.2 DFT analysis

DFT analysis as depicted in Table 1 shows the calculated parameters that reflect the reactivity and the stability of the B-CuO/rGO nanocomposite. These parameters were calculated via the Equations 1-7.

$$\Delta E = E_{LUMO} - E_{HOMO} \quad (1)$$

$$\chi = -\frac{1}{2}(E_{HOMO} + E_{LUMO}) \quad (2)$$

$$\eta = \frac{1}{2}(E_{LUMO} - E_{HOMO}) \quad (3)$$

$$\sigma = \frac{1}{\eta} \quad (4)$$

$$P_i = -X \quad (5)$$

$$\omega = \frac{P_i^2}{2} \quad (6)$$

$$\Delta N_{max} = -\frac{P_i}{\eta} \quad (7)$$

Figure 3 shows the 3D structure of the B-CuO/rGO nanocomposite used for DFT analysis. The energy difference between HOMO and LUMO was found to be 3.2 eV and was related to the bioactivity and stability of the nanocomposite because of  $n-\pi^*$  and  $\pi-\pi^*$  transitions due to the presence of C-C bonds and C=O group as reported previously [23, 24]. A previous study showed the size-dependent changes in the Density of States (DOS) of the nanocrystalline CdSe and the HOMO-LUMO energy gap revealed that the appearance of the discrete energy bands is due to the decrease in size and dimension [25]. The quantum confinement effect can give an insight into the optoelectronic and semiconducting properties of the NPs. Studying the 3D structure of B-CuO/rGO is important for drug design and understanding various therapeutic applications, as it has been previously shown that B-CuO and rGO both exhibit excellent biological activity [26]. General reactivity descriptors were found to be consistent with previous reports [27]. The order of stability also correlated with the overall hardness of the molecule (stability decreases as stiffness decreases), the value 1.604 eV indicated the increased stability of the B-CuO/rGO nanocomposite in line with previous literature [22, 28]. The important parameters which were calculated are discussed below:

#### 3.2.1 HOMO-LUMO gap

The analysis of the HOMO-LUMO gap in various nanocomposites offers valuable insights into their electrical characteristics. The HOMO and LUMO gap in the nanocomposite was observed to be 3.208 eV. The HOMO-LUMO gap of a semiconductor nanocrystal is directly proportional to its

size. With the decreasing size of the nanomaterials, the energy separation between the band-edge levels also increases. The electron affinity (EA) is also directly related to the energy of the LUMO because it inclines towards accepting electrons and therefore acts as an electron acceptor [29].

#### 3.2.2 Ionization potential (IP)

The ionization potential (IP) is directly proportional to the HOMO energy as the HOMO orbital tends to donate electrons and therefore acts as an electron donor [30, 31]. The ionization potential refers to the energy required to separate the electron from the cluster. The IP of the B-CuO/rGO nanocomposite was found to be 7.24 eV showing that it may take part in the chemical reactions.

#### 3.2.3 Absolute hardness and softness

The hardness is inversely proportional to the softness which is a property of a molecule that measures the extent of chemical reactivity.  $\eta$  and  $S$  are associated with the energy gap. Molecules with high energy gaps are generally hard, while those with small energy gaps are soft. The absolute hardness and softness of the nanocomposite were observed to be 1.6 and 0.62 eV respectively. The hardness and softness were calculated for the polarization of the nanocomposite showed it to be a hard acid.

#### 3.2.4 Absolute electronegativity

Electronegativity measures the power of an atom to attract electrons to it. Chemical potential on the other hand bears an inverse relationship with electronegativity. The calculated absolute electronegativity of B-CuO/rGO nanocomposite was 5.642 inferring that the nanocomposite was highly polar.

## 4. Conclusion

In this article, we have successfully studied the B-CuO/rGO nanocomposite, called the DFT-based definition concept and molecular docking. It is very important to comprehend the protein-metal binding and the complex formed during the interaction between nanomaterials and the biomolecules and that has led to the utility of molecular docking which predicts the cooperation affinity of the protein-metal complex and also the hindrances and limitations where the binding is not feasible. For the biomedical applications of nanomaterials, the applications of molecular docking are numerous, yet under-explored. From our calculations, it can be seen that the proposed B-CuO/rGO nanocomposite can be studied for medicinal and photocatalytic applications.

**Acknowledgements** The authors are thankful to the R & D cell of the Integral University, Lucknow for providing the Manuscript Communication Number (IU/R&D/2023-MCN0002060). They are also thankful to the Department of Applied Sciences, Indian Institute of Information Technology, Allahabad for providing support for the computational studies.



**Ethical Approval**

This manuscript does not report on or involve the use of any animal or human data or tissue. So the ethical approval does not applicable.

**Funding**

No funding was received to assist with conducting this study and the preparation of this manuscript.

**Authors Contributions**

All authors have contributed equally to prepare the paper.

**Availability of Data and Materials**

The data that support the findings of this study are available from the corresponding author upon reasonable request.

**Conflict of Interests**

The authors declare that they have no known competing financial interests or personal relationships that could have appeared to influence the work reported in this paper.

**Open Access**

This article is licensed under a Creative Commons Attribution 4.0 International License, which permits use, sharing, adaptation, distribution and reproduction in any medium or format, as long as you give appropriate credit to the original author(s) and the source, provide a link to the Creative Commons license, and indicate if changes were made. The images or other third party material in this article are included in the article's Creative Commons license, unless indicated otherwise in a credit line to the material. If material is not included in the article's Creative Commons license and your intended use is not permitted by statutory regulation or exceeds the permitted use, you will need to obtain permission directly from the OICCPublisher. To view a copy of this license, visit <https://creativecommons.org/licenses/by/4.0>.

**References**

- [1] S. Jabeen, N. Ahmad, S. Bala, D. Bano, and T. Khan. Nanotechnology in environmental sustainability and performance of nanomaterials in recalcitrant removal from contaminated Water: A review. *Int. J. Nano Dimens*, **14**:1–28, 2023. DOI: <https://doi.org/10.22034/IJND.2022.1963262.2162>.
- [2] S. Jabeen, A.S. Ganie, S. Bala, and T. Khan. Photocatalytic degradation of malachite green dye via an inner transition metal Oxide-based nanostructure fabricated through a hydrothermal route. *Mater. Proceedings*, **14**: 5–9, 2023. DOI: <https://doi.org/10.3390/IOC2023-14445>.
- [3] S. Jabeen, A.S. Ganie, N. Ahmad, S. Hijazi, S. Bala, D. Bano, and T. Khan. Fabrication and studies of LaFe<sub>2</sub>O<sub>3</sub>/Sb<sub>2</sub>O<sub>3</sub> heterojunction for enhanced degradation of Malachite green dye under visible light irradiation. *Inorg. Chem. Commun*, **152**:110729, 2023. DOI: <https://doi.org/10.1016/j.inoche.2023.110729>.
- [4] S. Siddique, M. Waseem, T. Naseem, A. Bibi, M. Hafeez, S.U. Din, S. Haq, and S. Qureshi. Photo-catalytic and anti-microbial activities of rGO/CuO nanocomposite. *J. Inorg. Organomet. Polym. Mater*, **31**:1359–1372, 2021. DOI: <https://doi.org/10.1007/s10904-020-01760-x>.
- [5] S. Esfahani, J. Akbari, S. Soleimani-Amiri, M. Mirzaei, and A.G. Gol. Assessing the drug delivery of ibuprofen by the assistance of metal-doped graphenes: Insights from density functional theory. *Diam. Relat. Mater*, **135**:109893, 2023. DOI: <https://doi.org/10.1016/j.diamond.2023.109893>.
- [6] S. Jabeen, V.U. Siddiqui, S. Rastogi, S. Srivastava, S. Bala, N. Ahmad, and T. Khan. Fabrication of B–CuO nanostructure and B–CuO/rGO binary nanocomposite: A comparative study in the context of photodegradation and antimicrobial activity assessment. *Mater. Today Chem*, **33**:101712, 2023. DOI: <https://doi.org/10.1016/j.mtchem.2023.101712>.
- [7] O. Akhavan and E. Ghaderi. Toxicity of graphene and graphene oxide nanowalls against bacteria. *ACS Nano*, **10**:5731–5733, 2010. DOI: <https://doi.org/10.1021/nn101390x>.
- [8] L. Ou, B. Song, H. Liang, J. Liu, X. Feng, B. Deng, and L. Shao. Toxicity of graphene-family nanoparticles: A general review of the origins and mechanisms. *Particle Fibre Toxicol*, **13**:1–24, 2016. DOI: <https://doi.org/10.1186/s12989-016-0168-y>.
- [9] T. Khan, I. Azad, R. Ahmad, A.J. Lawrence, M. Azam, S.M. Wabaidur, S.I. Al-Resayes, S. Raza, and A.R. Khan. Molecular structure simulation of (E)-2-(butan-2-ylidene) hydrazinecarbothioamide using the DFT approach, and antioxidant potential assessment of its complexes. *King Saud. Univ. Sci*, **33**:101313, 2021. DOI: <https://doi.org/10.1002/vjch.202200233>.
- [10] D. Selli, G. Fazio, and C. Di Valentin. Using density functional theory to model realistic TiO<sub>2</sub> nanoparticles, their photoactivation, and interaction with water. *Catalysts*, **7**:357–362, 2017. DOI: <https://doi.org/10.3390/catal7120357>.
- [11] M. Bursch, J.M. Mewes, A. Hansen, and S. Grimme. Best-practice DFT protocols for basic molecular computational chemistry. *Angew. Chem. Int. Ed*, **61**:e202205735, 2022. DOI: <https://doi.org/10.1002/anie.202205735>.
- [12] P.A. Ghamsari, M. Samadzadeh, and M. Mirzaei. Halogenated derivatives of cytidine: Structural analysis and binding affinity. *Theor.*

- Comput. Chem.*, **19**:2050033, 2020. DOI: <https://doi.org/10.1142/S0219633620500339>.
- [13] T.J. MacCormack, R.J. Clark, M.K. Dang, G. Ma, J.A. Kelly, J.G. Veinot, and G.G. Goss. Inhibition of enzyme activity by nanomaterials: potential mechanisms and implications for nanotoxicity testing. *Nanotoxicol.*, **6**:514–525, 2012. DOI: <https://doi.org/10.3109/17435390.2011.587904>.
- [14] D.I. Sánchez-Machado, J. López-Cervantes, R. Sendón, and A. Sanches-Silva. Aloe vera: Ancient knowledge with new frontiers. *Trends Food Sci. Technol.*, **61**:94–102, 2017. DOI: <https://doi.org/10.1016/j.tifs.2016.12.005>.
- [15] S. Dacrory. Antimicrobial activity, DFT calculations, and molecular docking of dialdehyde cellulose/graphene oxide film against COVID-19. *J. Polym. Environ.*, **29**:2248–2260, 2021. DOI: <https://doi.org/10.1007/s10924-020-02039-5>.
- [16] M. Aghaei, M. Mirzaei, M. Ghanadian, M. Fallah, and R. Mahboodi. 6-Methoxylated flavonoids: Jacein, and 3-demethyljacein from *Centaurea schmidii* with their endoplasmic reticulum stress and apoptotic cell death in breast cancer cells along with in-silico analysis. *Iran. J. Pharm. Res.*, **20**:417–422, 2021. DOI: <https://doi.org/10.22037/ijpr.2020.113895.14548>.
- [17] T. Khan, A.J. Lawrence, I. Azad, S. Raza, and A.R. Khan. Molecular docking simulation with special reference to flexible docking approach. *JSM Chem.*, **6**:1053–1058, 2019. DOI: <https://doi.org/10.47739/2334-1831/1053>.
- [18] M.D. Hanwell, D.E. Curtis, D.C. Lonie, T. Vandermeersch, E. Zurek, and G.R. Hutchison. Avogadro: An advanced semantic chemical editor, visualization, and analysis platform. *J. Cheminfo.*, **4**:1–17, 2012. DOI: <https://doi.org/10.1186/1758-2946-4-17>.
- [19] K. Remans, K. Pauwels, P. van Ulsen, L. Buts, P. Cornelis, J. Tommassen, and P. Van Gelder. Hydrophobic surface patches on LolA of *Pseudomonas aeruginosa* are essential for lipoprotein binding. *J. Mol. Biol.*, **401**:921–930, 2010. DOI: <https://doi.org/10.1016/j.jmb.2010.06.067>.
- [20] A.B. Gurung, A. Bhattacharjee, and M.A. Ali. Exploring the physicochemical profile and the binding patterns of selected novel anticancer Himalayan plant-derived active compounds with macromolecular targets. *Info. Med. Unlocked.*, **5**:1–14, 2016. DOI: <https://doi.org/10.1016/j.imu.2016.09.004>.
- [21] S.Y. Tanaka, S.I. Narita, and H. Tokuda. Characterization of the *pseudomonas aeruginosa* Lol system as a lipoprotein sorting mechanism. *J. Biol. Chem.*, **282**:13379–13384, 2007. DOI: <https://doi.org/10.1074/jbc.M611840200>.
- [22] R. Akilan, S. Vinnarasi, S. Mohanapriya, and R. Shankar. Reconnoitering the nature of interaction and effect of electric field on Pd/Pt/Ni decorated 5-8-5/55–77 defected graphene sheet for hydrogen storage. *Int. J. Hydrogen Energy.*, **45**:744–763, 2020. DOI: <https://doi.org/10.1016/j.ijhydene.2019.10.170>.
- [23] S. Sagadevan, J.A. Lett, G.K. Weldegebrial, S. Garg, W.C. Oh, N.A. Hamizi, and M.R. Johan. Enhanced photocatalytic activity of rGO-CuO nanocomposites for the degradation of organic pollutants. *Catalysts*, **11**:1008–1011, 2021. DOI: <https://doi.org/10.3390/catal11081008>.
- [24] G.D. Varma. Enhanced room temperature sensitivity of Ag-CuO nanobrick/reduced graphene oxide composite for NO<sub>2</sub>. *J. Alloys Compd.*, **806**:1469–1480, 2019. DOI: <https://doi.org/10.1016/j.jallcom.2019.07.355>.
- [25] F.T. Rabouw and C. de Mello Donega. Book: Handbook of photoactive semiconductor nanocrystal quantum Dots. ISBN: 978-3-319-51191-7, 2017. DOI: <https://doi.org/10.1007/978-3-319-51192-4>.
- [26] S.E. Elugoke, O.E. Fayemi, A.S. Adekunle, B.B. Mamba, T.T. Nkambule, and E.E. Ebenso. Electrochemical sensor for the detection of dopamine using carbon quantum dots/copper oxide nanocomposite modified electrode. *Flat. Chem.*, **33**:100372, 2022. DOI: <https://doi.org/10.1016/j.flatc.2022.100372>.
- [27] R. Ahmadi and S. IZANLOO. Development of HAp/GO/Ag coating on 316 LVM implant for medical applications. *J. Mech. Behav. Biomed. Mater.*, **126**:105075, 2022. DOI: <https://doi.org/10.1016/j.jmbbm.2022.105075>.
- [28] A. Khan, F. Khan, M. Shahwan, M.S. Khan, F.M. Husain, M.T. Rehman, M.I. Hassan, A. Islam, and A. Shamsi. Mechanistic insight into the binding of graphene oxide with human serum albumin: Multispectroscopic and molecular docking approach. *Spectrochim. Acta A Mol Biomol. Spectrosc.*, **256**:119750, 2021. DOI: <https://doi.org/10.1016/j.saa.2021.119750>.
- [29] P. Makkar and N.N. Ghosh. A review on the use of DFT for the prediction of the properties of nanomaterials. *RSC Adv.*, **11**:27897–27924, 2021. DOI: <https://doi.org/10.1016/j.saa.2021.119750>.
- [30] Y.T. Assatse, G.W. Ejuh, F. Tchoffo, and J.M.B. Ndjaka. DFT studies of nanomaterials designed by the functionalization of modified carboxylated carbon nanotubes with biguanide derivatives for nanomedical, nonlinear and electronic applications. *Chinese J. Phy.*, **58**:253–262, 2019. DOI: <https://doi.org/10.1016/j.cjph.2019.01.014>.
- [31] M.A. Sadjadi, B. Sadeghi, and K. Zare. Natural bond orbital (NBO) population analysis of cyclic thionylphosphazenes, [NSOX (NPCl<sub>2</sub>)<sub>2</sub>]; X = F (1), X

= C1 (2). *J. Mol. Str.:THEOCHEM*, **817**:27–33, 2007.  
DOI: <https://doi.org/10.1016/j.theochem.2007.04.015>.